Journal of Catalysis **189,** 360–369 (2000)
doi:10.1006/jcat.1999.2717, available online at http://www.idealibrary.com on IDEAL®

Kinetics of the Photocatalytic Oxidation of Gaseous Acetone over Platinized Titanium Dioxide

A. V. Vorontsov,*,[1] I. V. Stoyanova,* D. V. Kozlov,† V. I. Simagina,* and E. N. Savinov*

*Boreskov Institute of Catalysis, pr. Ak. Lavrentieva 5, Novosibirsk 630090, Russian Federation; and †Novosibirsk State University, Pirogova 2, Novosibirsk 630090, Russian Federation

Received May 18, 1999; revised September 24, 1999; accepted September 28, 1999

The photocatalytic oxidation of acetone is investigated in a flow-circulating reactor over Pt/TiO_2 prepared by photodeposition (Pt/TiO_2-P) as well as by reduction with $NaBH_4$ (Pt/TiO_2-C). Compared to untreated TiO_2, Pt/TiO_2-P is less active and Pt/TiO_2-C more active at 40–120°C, water concentration of 4500 ppm, and light intensity of 1.10×10^{-6} E/(min cm^2). The increased activity of Pt/TiO_2-C is related to the stronger adsorption of acetone and higher rate constant, as revealed by dependence of the reaction rate on concentration. Adsorption constants obtained from adsorption isotherms are significantly lower than those constants obtained from the dependence of the rate on acetone concentration. This suggests the presence of acetone photoadsorption during photocatalytic oxidation. Platinized samples did not demonstrate steady state deactivation, which was observed over TiO_2 at temperatures above 100°C. However, there was a decrease in the oxidation rate while reaching steady state after an increase of temperature to 80°C and above. Apparent activation energy of photocatalytic oxidation over platinized samples was 10–13 kJ/mol; the apparent activation energy of thermal acetone oxidation was 84 kJ/mol for Pt/TiO_2-P and about 40 kJ/mol for Pt/TiO_2-C. At 80–140°C, photoinduced oxidation could occur on Pt particles, as shown by acetone photoinduced oxidation over Pt/γ-Al_2O_3. The lack of deactivation of Pt/TiO_2 above 100°C may be related to the modification of the TiO_2 surface during Pt deposition because TiO_2 treated with $NaBH_4$ demonstrated a higher deactivation temperature. The dependence of activity on Pt content in Pt/TiO_2-C had a peak at Pt content of about 0.1 wt%. The TiO_2 used in this study had higher adsorption and rate constants compared to TiO_2 Degussa P25. An estimate showed that there were no concentration gradients inside the photocatalyst film under experimental conditions of this study.

INTRODUCTION

Recent studies on photocatalytic oxidation demonstrated that this type of reaction enables the decontamination of the environment. Photocatalytic purification has a number of advantages for treating water and air, especially for the removal of organic admixtures. A significant rate of oxidation which results in simple inorganic molecules, and a low selectivity toward a variety of compounds make photocatalysis an attractive means for the solution of environmental problems.

Titanium dioxide proved to be the most active semiconductor photocatalyst for oxidative reactions. The search for photocatalysts that are even more active revealed that deposition of platinum could appreciably improve the photocatalytic activity of TiO_2.

Platinized titanium dioxide was originally designed for photocatalytic water decomposition (1–4) because titanium dioxide alone does not photocatalyze this reaction. Platinum deposits are believed to cause better separation of photogenerated charge carriers, with electrons being collected in platinum particles. Owing to this enhanced charge separation, Pt/TiO_2 is able to photocatalyze various electrochemical reactions, for instance, water decomposition, the Kolbe reaction (5), reduction of nitrate ions (6), and reduction of chromium(IV) (7). On the other hand, platinum is an excellent thermal catalyst. The properties of platinum as a catalyst, together with the photoelectrochemical behavior of the Pt/TiO_2 interface, give rise to unusual reactions such as photocatalytic hydrogenation with water (8) and hydrogen photocatalytic isotopic exchange (9, 10). Reactions of gas-phase photocatalytic oxidation do not require photoelectrochemical conditions. This is corroborated by the fact that an increase in water vapour pressure usually has an adverse effect on the reaction rate (11, 12), except when the deactivation of TiO_2 occurs (11–13) or when water is one of the reactants (13, 14). Gas-phase oxidation by oxygen consumes both photogenerated electrons and holes because neither the initial organic molecules nor the product molecules are charged. When photogenerated charges have large distances between them, intermediates of oxidation must move from the electron sites to those of the hole and back for the reaction to take place. This can decrease the quantum yield since photogenerated charges can accumulate in excess and recombine. Therefore, better charge separation in Pt/TiO_2 hardly causes its increased oxidative photocatalytic activity. Recent studies on ethanol and acetaldehyde gas-phase photocatalytic oxidation (15, 16)

[1] To whom correspondence should be addressed. E-mail: voronts@catalysis.nsk.su.

0021-9517/00 $35.00

emphasized the role of thermal catalytic reactions in overall oxidation processes over TiO_2 and Pt/TiO_2. In particular, Kennedy and Datye (15) suggested that the photothermal synergistic effect observed over Pt/TiO_2 for ethanol oxidation is a result of a mixed series-parallel kinetics. The latter includes gas-phase transport of acetaldehyde, a product of ethanol photooxidation over TiO_2, to Pt where it oxidizes completely in thermal reactions. Falconer and Magrini-Bair (16) attributed an increased photocatalytic activity at elevated temperatures of Pt/TiO_2, compared to TiO_2, to spillover of oxygen from Pt to TiO_2.

In this paper we present experimental results and propose two other reasons for the enhanced photocatalytic activity of Pt/TiO_2. They include photostimulated oxidation on the surface of Pt particles and stronger adsorption of organic molecules on platinized TiO_2 compared to pure TiO_2.

Fu *et al.* showed that Pt/TiO_2, prepared by reduction of H_2PtCl_6 with $NaBH_4$, has much higher activity in benzene oxidation (17). However, many other researchers (2–4, 6, 15, 16, 18) employed Pt/TiO_2 prepared by photocatalytic deposition. It was shown recently that photodeposition can lead to platinum in various chemical states (Pt^0, PtO_2, and $Pt(OH)_2$) depending on the conditions of deposition (19); Pt^0/TiO_2 has the highest photocatalytic activity in acetone oxidation (20). In the current study we compare photocatalytic activity of Pt^0/TiO_2 samples, prepared by $NaBH_4$ reduction, and photodeposition. The method of preparation that gave the more active photocatalyst was then used to prepare samples to determine the causes of their high activity. Finally, the platinum content that gave the highest rate of acetone photocatalytic oxidation at near ambient temperature was determined.

EXPERIMENTAL

The preparation of titanium dioxide was reported previously (12). It was made by aqueous hydrolysis of chemically pure $TiCl_4$ and precipitated by NaOH. The deposit was washed thoroughly with distilled water and calcined in air at 400°C for 3 h. A TEM micrograph of this titania revealed that primary particles show high crystallinity with a typical size of 8–13 nm and form larger aggregates of 300–800 nm. The specific surface area of this photocatalyst was 123 ± 3 m^2/g, as determined using low-temperature nitrogen adsorption in an ASAP-2400 instrument (Micromeritics). X-ray analysis revealed the existence of the anatase phase only.

Titania prepared in this manner was loaded with platinum using two different methods of H_2PtCl_6 reduction: photocatalysis and reduction with $NaBH_4$. In this paper, samples prepared by reduction with $NaBH_4$ are designated "C" and those prepared photocatalytically are designated "P." P or C is followed by the weight percentage of Pt. When the different methods of Pt determination used gave distinct contents, a mean value is used in the designation. The samples used are listed in Table 1. Deposition of platinum did not result in significant changes of the specific surface area. Sample C0.41 had a specific surface of 128 ± 3 m^2/g. Distributions of pore volume and pore surface area in this sample had peaks at pore diameters of about 11 and 10 nm, respectively. These values are close to the primary particle diameter and correspond to pores formed by primary titania particles.

For photocatalytic deposition (sample P0.9), 19 ml of 0.1 M acetic acid and 1.32 ml of 0.077 M H_2PtCl_6 were added to 2 g of TiO_2. The pH of the suspension was adjusted to 4.0 by the addition of NaOH solution. The suspension was irradiated in a quartz reactor by a 250-W Xe lamp, 12 cm from the reactor, for 5 h. Then, the catalyst was washed by decantation to free it of Cl^- and dried in air at 100°C for 4.5 h.

Samples C0.08–C0.76 were loaded with Pt by reduction with $NaBH_4$. Titanium dioxide was impregnated with an estimated quantity of aqueous solution of H_2PtCl_6 to incipient wetness. TiO_2 with adsorbed H_2PtCl_6 was treated with

TABLE 1

Photocatalysts Studied

Designation	Composition	Platinum deposition method	Objective Pt content (wt%)	Pt content determined by	
				X-ray fluorescence	Spectrophotometrically
TiO_2	TiO_2	—	—	—	—
P0.9	Pt/TiO_2	photocatalytic	1.0	0.9	—
C0.00	TiO_2	$NaBH_4$ reduction	0.00	—	—
C0.08	Pt/TiO_2	$NaBH_4$ reduction	0.1	0.07	0.09
C0.09	Pt/TiO_2	$NaBH_4$ reduction	0.2	0.08	0.10
C0.11	Pt/TiO_2	$NaBH_4$ reduction	0.3	0.10	0.12
C0.41	Pt/TiO_2	$NaBH_4$ reduction	0.5	0.40	0.42
C0.76	Pt/TiO_2	$NaBH_4$ reduction	1.0	0.78	0.74
C100	Pt	$NaBH_4$ reduction	100	—	—
Pt/Al_2O_3	$Pt/\gamma\text{-}Al_2O_3$	$NaBH_4$ reduction	0.5	—	—

a 3-fold excess of an aqueous solution of $NaBH_4$. Then, the sample was washed thoroughly with distilled water, filtered, and dried at 90°C in air. Sample C0.00 was prepared using the same method as that for C0.41 but without adding H_2PtCl_6. Platinization of γ-Al_2O_3 was carried out according to the same method. The specific surface area of γ-Al_2O_3, as determined by BET, was 115 m^2/g. Sample C100 was platinum black prepared by the reduction of H_2PtCl_6 with $NaBH_4$. The size of the Pt particles in all samples with composition Pt/TiO_2 was below 1 nm because the particles could not be detected by TEM.

The platinum content was ascertained by two methods. X-ray fluorescence analysis was performed with a VRA-20 instrument with a W anode in the X-ray tube. The other method was spectrophotometric determination with $SnCl_2$.

Pt/TiO_2 samples showed a noticeable difference between the objective and actual platinum contents, which could result when some of the Pt particles are removed during washing with water. To prove this, the solution, after sample C0.41 was washed, was analyzed by atomic absorption spectroscopy (AAS). The result indicates that about 0.1 wt% of platinum resides in the washing solution. This means that the difference was completely due to the removal of Pt during washing. According to AAS analysis of the washing solution, the content of Na from $NaBH_4$ in C0.41 was below 0.1 wt%. The difference between the objective and actual platinum content was higher for chemically loaded samples. We expect that reduction with $NaBH_4$ will produce many Pt particles, which are not attached to TiO_2 particles. On the contrary, photocatalytic reduction requires close contact between Pt and TiO_2 and, therefore, produces few unattached Pt particles. Very small Pt particles that are not attached to TiO_2 agglomerates can be easily washed out.

UV–vis diffuse reflectance spectra of the catalysts were recorded using a Shimadzu UV-300 spectrophotometer (Japan) equipped with an integrating sphere appliance. MgO was a reference sample, and its reflectance was assumed to be 85%.

Kinetic measurements were performed in a flow-circulation system described in detail elsewhere (21). The flow-circulation system includes a quartz reactor, a membrane circulation pump, and stainless steel connection pipes. The reactor was placed in a temperature-controlled box to maintain the necessary temperature between 40 and 140°C. The circulation rate was about 8 L/min, more than 100 times higher than the selected maximum input flow rate. Therefore, the reactor can be considered as a perfect stirring reactor without concentration and temperature gradients.

Oxygen in air was used as the oxidant. Input gas flow was prepared according to the following procedure. Purified air from the air line was divided into three flows. One was passed through a saturator filled with water to attain necessary water vapour concentration, while the second flow was passed through a saturator with acetone. The third flow was used to dilute the gas mixture produced after the confluence of all the flows.

Input and output gas mixtures were analyzed using gas chromatographs equipped with a FID and TCD. Carbon dioxide was determined by analyzing methane on FID after methanation of a gas sample.

For the tests of activity, catalysts were applied to glass plates from aqueous slurries to cover an area of 3 cm^2. The thickness of the catalyst layer was sufficient to absorb all incident UV light.

Samples in the quartz reactor incorporated in the flow-circulation loop were irradiated by the light of a 1000-W xenon lamp transmitted through a 313-nm interference filter. The incident light intensity was 7 mW/cm^2, or 1.10×10^{-6} E/(min cm^2).

The rate of acetone oxidation was calculated from the rate of CO_2 production, the product of its complete oxidation. Measurements of the CO_2 concentrations were made until steady state was reached; steady state measurements only were used to calculate the oxidation rate, except for the experiments that showed how the steady state was reached. Steady state was usually reached in about 30 min. No other carbon-containing products were detected during the experiments.

Isotherms of acetone adsorption were measured in a thermostatic 160-ml glass vessel equipped with ports for purging air with controlled humidity and injection of liquid acetone. Powder of the catalysts was distributed uniformly on the bottom of the vessel. The vessel with the catalyst was purged with air for 24 h, and then definite volumes of liquid acetone were injected and resultant equilibrium concentration was measured.

RESULTS AND DISCUSSION

Since the pure and platinized titania samples were prepared for use in a photocatalytic reaction, their reflective properties may have had a strong effect on the photocatalytic activity. Figure 1 shows diffuse reflectance spectra of pure and platinized TiO_2 and of platinum black. The presence of Pt clearly changes the spectrum of TiO_2 in the visible light region. The increase in the Pt content reduces the reflectance. The sample C0.00, which was treated with $NaBH_4$ without adding H_2PtCl_6, has a spectrum that is almost identical to that of the initial TiO_2. Just after the addition of $NaBH_4$, C0.00 turned gray and then slowly turned white when washed with water and while it was drying. Therefore, this sample seems to be completely reoxidized during preparation. It is interesting to compare the diffuse reflectance spectra of different titanias with similar platinum content. Previous work (20) used TiO_2 (Fluka) with primary particles with an average size of 160 nm, whereas in this study we used TiO_2 with primary particles of 8–13 nm. Nevertheless, after approximately 0.8 wt% Pt was loaded,

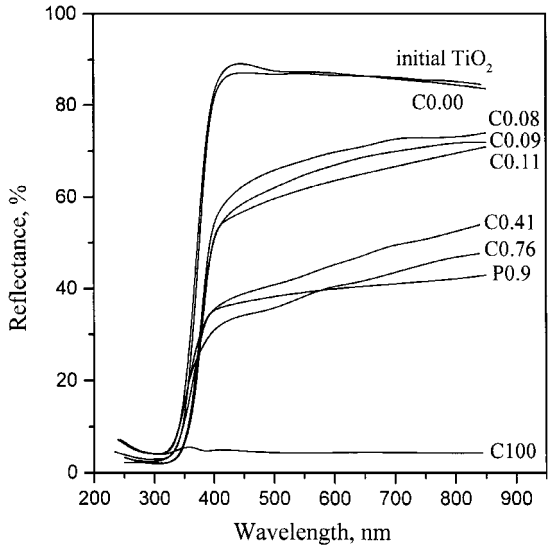

FIG. 1. Diffuse reflectance spectra of the photocatalysts studied.

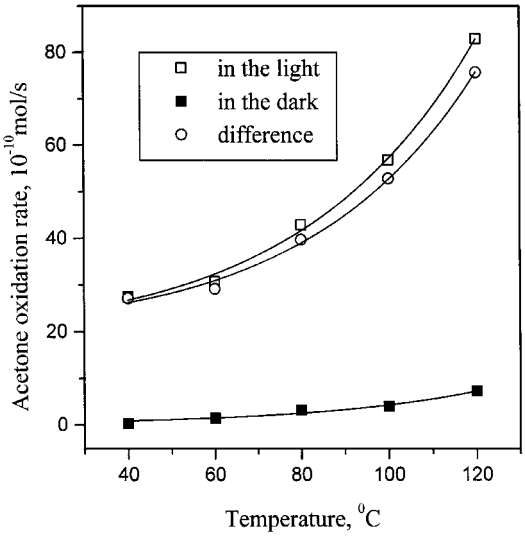

FIG. 3. Temperature dependence of the acetone oxidation rate over sample C0.76. Weight of catalyst 21.9 mg; acetone concentration 560 ppm; water vapor concentration 4500 ppm.

either by photocatalysis or $NaBH_4$ reduction, both samples showed similar spectra with reflectance near 40% in the visible light region. These samples contained platinum particles of different sizes: 3 nm for TiO_2 (Fluka) and <1 nm for current TiO_2. The similarity of their spectra can be understood if one assumes that the platinum particles are translucent for visible light and that the characteristic depth of penetration in both samples of TiO_2 is the same. In this case, the fraction of visible light absorbed was the same for both samples.

Figure 2 demonstrates the temperature dependence of the rate of acetone oxidation over Pt/TiO_2 P0.9. The rate of thermal acetone oxidation is already considerable at temperatures above 80°C. The rate of photocatalytic and thermal oxidation increases steadily with increasing temperature and is satisfactorily approximated by an exponential dependence (Fig. 2). The apparent activation energy is 10.4 ± 3.1 kJ/mol for photocatalytic oxidation and 84.0 ± 1.9 kJ/mol for thermocatalytic oxidation. Compared to unplatinized TiO_2 (12), the rate of acetone oxidation on P0.9 is 1.5 times lower at 40°C, but is slightly higher at 100°C. However, the rate of purely photocatalytic oxidation over P0.9 is lower, even at 100°C.

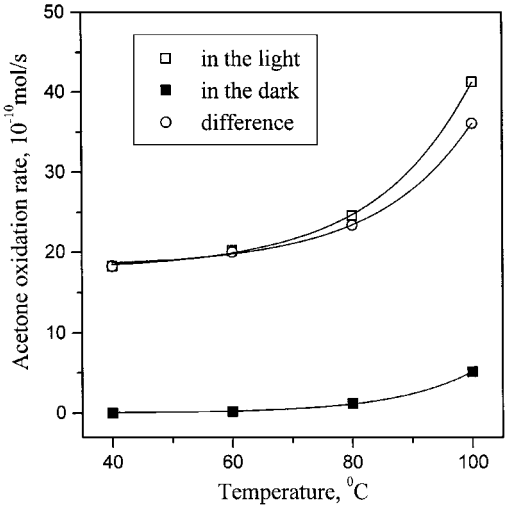

FIG. 2. Temperature dependence of the acetone oxidation rate over sample P0.9. Weight of catalyst 30.45 mg; acetone concentration 560 ppm; water vapor concentration 4100 ppm.

Sample C0.76 with a similar platinum content exhibits better activity during acetone oxidation (Fig. 3). At all temperatures from 40 to 120°C, the rate of acetone oxidation is higher over C0.76 than over TiO_2. The greatest difference by 2.7 is observed at 120°C. At this temperature, the rate of oxidation over TiO_2 begins to decrease, whereas there is no sign of a decrease over C0.76.

Obviously, chemical deposition of Pt produced a more active photocatalyst than photocatalytic deposition. The rate of thermal acetone oxidation over C0.76 at 100°C (1.83×10^{-8} mol/(s g)) is also higher than that over P0.9 (1.70×10^{-8} mol/(s g)). This suggests that the Pt particles in C0.76 were smaller than those in P0.9, assuming that acetone oxidation is a structure-insensitive reaction. The apparent activation energy is 13.3 ± 2.0 kJ/mol for photocatalytic oxidation and 38.1 ± 6.1 kJ/mol for thermocatalytic oxidation. In comparison with the photocatalytically prepared sample, the apparent activation energy of thermal oxidation is twice as low.

Although the temperature dependence of acetone oxidation over C0.76 does not demonstrate deactivation, the time to reach steady state at 120°C is markedly longer than that at lower temperatures. A temporal profile of activity is depicted in Fig. 4A. There is a considerable decrease in the

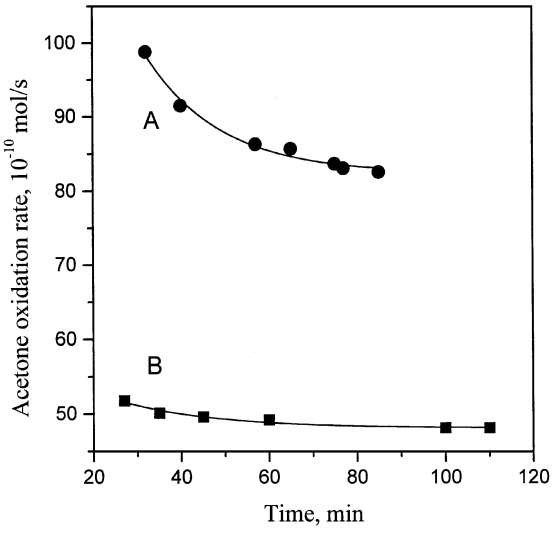

FIG. 4. Decrease in the acetone oxidation rate after an increase in temperature: (A) From 40 to 120°C over C0.76. Conditions are the same as those reported in Fig. 3. (B) From 60 to 80°C over C0.41. Conditions are the same as those reported in Fig. 5.

oxidation rate after an increase in temperature to 120°C. It is interesting that the time to reach steady state over C0.76 is similar to that over TiO_2 (12), approximately 80 min. The nature of deactivation on both catalysts appears to be the same: accumulation of intermediate products on the TiO_2 surface. However, it was difficult to detect the brown color after operation at 120°C in C0.76 because it was initially dark gray.

Luo and Falconer (22) revealed that acetone undergoes aldol condensation and cyclization reactions on TiO_2 Degussa P25. They found that in dry conditions mesityl oxide begins to desorb at about 130°C from TiO_2 with acetone saturation coverage. About 10% of the surface acetone was converted to strongly bound species that could not be removed by heating to 450°C. Such condensation products may be responsible for thermal deactivation of titania catalysts during photocatalytic oxidation of acetone. Mesityl oxide was not detected in our studies. This may be related to a lower rate of aldolization over given TiO_2. We used nonzero water concentrations. Water was reported to decrease the rate of aldolization by poisoning Lewis acid sites (23) that are active sites for aldolization over TiO_2 (24). Platinized TiO_2 does not demonstrate thermal deactivation, evidently due to maintaining (photo)thermal oxidation on Pt particles.

The platinum content can markedly influence the kinetics of photocatalytic oxidation (15). Therefore, temperature dependence was also measured for the sample with a lower platinum content. The dependence of C0.41 is shown in Fig. 5. In the temperature range of 40–80°C, this catalyst is more active photocatalytically than C0.76. However, at 100 and 120°C their photocatalytic activity was almost identical. Temperature dependency (Fig. 5) is a good fit to an exponential function represented by curves. The apparent activation energy is 11.5 ± 1.8 kJ/mol for photocatalytic oxidation and 43.7 ± 3.3 kJ/mol for thermocatalytic oxidation. There is no significant difference in the activation energies with C0.76 and C0.41. A pronounced difference between the apparent activation energy of photocatalytic and thermocatalytic oxidation suggests that their mechanisms are different. The final steps of thermocatalytic oxidation take place on Pt, presumably with the participation of acetone as well as some products of its oxidation/aldolization on TiO_2.

Assuming structure insensitivity of acetone thermal oxidation on Pt, an attempt was made to predict its rate over C0.41 based on the rate over C0.76. If the size of the Pt particles remains the same and if the Pt content affects only their number, then the rate would be directly proportional to the Pt content that would result in 0.99×10^{-8} mol/(s g). If the platinum content causes a change in the size of the Pt particles but does not change their number, then the rate would be proportional to the Pt content to the power of $\frac{2}{3}$ and would result in 1.21×10^{-8} mol/(s g). The actual rate of 1.35×10^{-8} mol/(s g) is greater than the results of both predictions. Taking the experimental error of 10% into account, we conclude that the second prediction gave a satisfactory result. Therefore, we anticipate that an increase in the Pt content will lead to the growth of the Pt particles.

Unplatinized TiO_2 showed signs of deactivation at temperatures exceeding 90°C (12). At lower temperatures, steady state was reached within 30 min. The situation is different for platinized TiO_2. Figure 4B shows the temporal profile of the acetone oxidation rate over C0.41 during the first minutes of operation at 80°C. The reaction rate

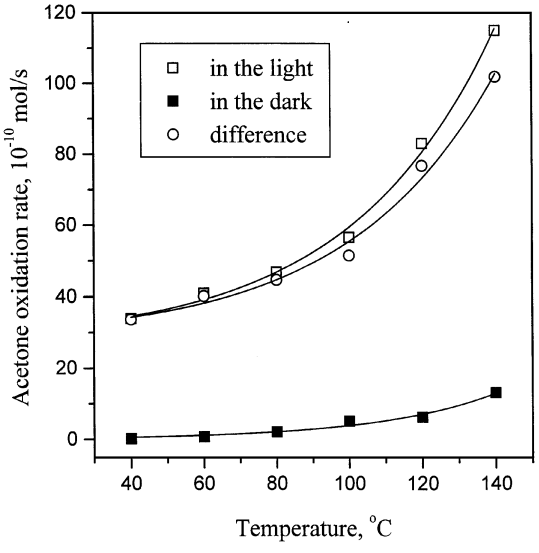

FIG. 5. Temperature dependence of the acetone oxidation rate over C0.41. Weight of catalyst 38 mg; acetone concentration 530 ppm; water vapor concentration 4500 ppm.

decreases by about 8%. Therefore, platinum induces some decay of Pt/TiO_2 activity at low temperatures. Since deactivation probably results from an excess of surface products, this behavior may be caused by the generation of products of acetone aldolization on TiO_2 that are oxidized at a lower rate than acetone on Pt clusters.

We study further the kinetics of acetone oxidation over platinized titania by considering the influence of the preparation method on the activity of TiO_2. Sample C0.00 was prepared using the same quantity of $NaBH_4$ as was used for C0.41 but without the addition of Pt. Thus, any differences in the kinetics of acetone oxidation over C0.00 and TiO_2 originate from this reductive treatment. Figure 6 shows the rate of acetone oxidation over C0.00 as a function of temperature. Compared with initial TiO_2 (12), the rate of oxidation is noticeably lower at 40 and 60°C. However, the rate is almost the same at 80°C and is higher at 100°C and above. Thermal deactivation of C0.00 begins at temperatures above 120°C and is less. Treatment with $NaBH_4$ evidently modified the TiO_2 surface, making it more resistant to thermal deactivation. Boron and sodium species in the adsorbed state probably prevent TiO_2 from being poisoned by partial oxidation products. Reaction of aldolization takes place on Ti^{4+} sites that can be blocked by sodium and boron species. Photocatalytic oxidation takes place also over surface hydroxyl groups and thus is not significantly inhibited. This testifies to the possibility of a beneficial effect of TiO_2 surface modification during Pt deposition.

The contribution of Pt to the total oxidation rate of acetone on Pt/TiO_2 was checked using Pt deposited on γ-Al_2O_3, a photocatalytically inactive support with a high specific surface area (115 m^2/g). Unsupported Pt (5 mg of sample C100) showed very low activity (rate $<5\times$ 10^{-11} mol/s) during acetone oxidation at 100°C. The temperature dependence of dark and illuminated acetone oxidation over Pt/Al_2O_3 is shown in Fig. 7. The rates under dark and illuminated conditions are equal at temperatures from 40 to 80°C. However, at higher temperatures, there is a considerable difference in these rates. From 80 to 100°C, the rates of dark and illuminated oxidation increase sharply with temperature, from 100 to 120°C the rates decrease with temperature, and at higher temperatures they increase again. This unusual behavior might be related to temperature changes in the catalyst, namely, agglomeration of Pt particles. Another possible cause is aldol condensation on alumina. It is known that condensation of acetone on alumina can start at as low temperature as −60°C (25). Products of aldol condensation are rather huge molecules which, if adsorbed on small Pt clusters, may prevent the chemisorption of oxygen and retard the oxidation. The noticeable difference between the oxidation rate in the dark and that in the light suggests the existence of light-stimulated acetone oxidation on Pt. The influence of radiation on reactions over metals is not new. The oxidation of CO on Pd is accelerated in UV light from 110 to 170°C (26); no acceleration was found at lower temperatures. The nature of this phenomenon is not clear. It may to some extend be due to the heating of Pt particles in the light, or due to surface photochemical oxidation of acetone. In Pt/TiO_2, UV light is absorbed predominantly by TiO_2, and only some of the UV light is absorbed by Pt. Therefore, a photostimulated reaction over Pt particles in Pt/TiO_2 may make a smaller contribution to the overall oxidation rate in comparison with that in Pt/Al_2O_3.

Thus, the overall process of acetone photocatalytic oxidation over Pt/TiO_2 at temperatures of 40–140°C includes

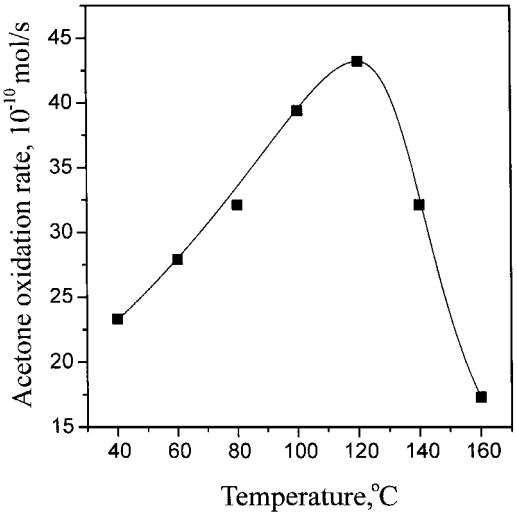

FIG. 6. Change in acetone oxidation rate with temperature over sample C0.00. Acetone concentration 590 ppm; water vapor concentration 4200 ppm.

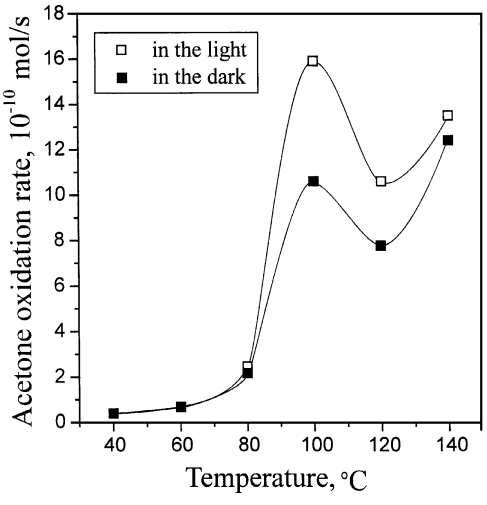

FIG. 7. Rate of acetone oxidation over Pt/Al_2O_3 as a function of temperature. Weight of catalyst 37 mg; acetone concentration 600 ppm; water vapor concentration 4500 ppm.

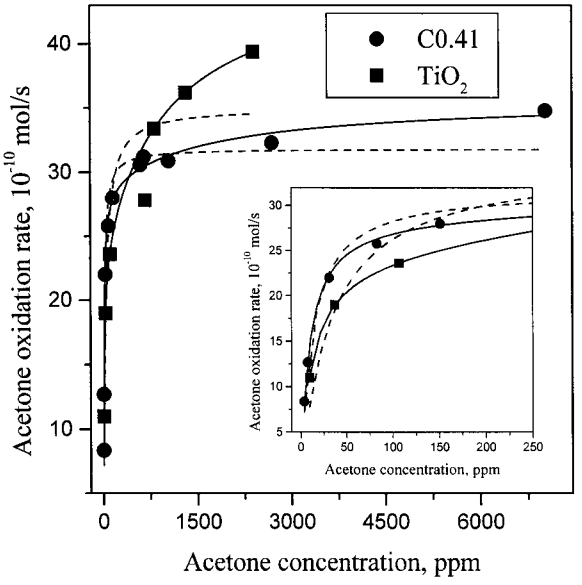

FIG. 8. Influence of acetone concentration on the acetone oxidation rate over TiO_2 and C0.41. Solid curves are the two-site LH model; dashed curves are the one-site LH model. The inset shows a magnified part of the graph at low acetone concentrations. Weight of catalysts 25 mg; temperature 40°C; water vapor concentration 4500 ppm.

seven reactions. Three dark reactions are oxidation of acetone to CO_2 over Pt, formation of poisoning products over TiO_2, and oxidation of poisoning products over Pt. Four photostimulated reactions are oxidation of acetone to CO_2 over TiO_2, oxidation of acetone to CO_2 over Pt, and oxidation of poisoning products over TiO_2 and over Pt.

We continued our study of the causes of the higher activity of platinized titania by measuring the dependence of the acetone oxidation rate for TiO_2 and the sample C0.41 on concentration (Fig. 8). We recently reported (12) that a good approximation of the dependence of the oxidation rate on acetone concentration for a given TiO_2 can be obtained by the Langmuir–Hinshelwood (LH) equation with two types of adsorption sites—surface hydroxyl groups and Ti^{4+} ions:

$$R = \frac{k_1 K_1 C_a}{1 + K_1 C_a} + \frac{k_2 K_2 C_a}{1 + K_2 C_a}. \qquad [1]$$

This equation was used to plot the solid curves in Fig. 8. The dashed curves represent the results of the fit by the one-site LH equation. Evidently, the one-site model does not fit the experimental data satisfactorily. The values of the corresponding parameters for the two-site model are listed in Table 2. The dependency of the rate on concentration is different for platinized and unplatinized TiO_2. At low acetone concentrations, the rate is higher over C0.41, but the situation is reverse at high concentrations. In C0.41, there should be three different types of adsorption sites: Pt clusters, Ti^{4+}, and surface OH groups. However, Eq. [1] describes the rate vs concentration well, and the introduction of the third term

TABLE 2

Parameters of Langmuir–Hinshelwood Equation for Curves in Fig. 8

Sample	k_1 (10^{-10} mol/s)	K_1 (ppm^{-1})	k_2 (10^{-10} mol/s)	K_2 (ppm^{-1})
TiO_2	23.8 ± 0.4	0.088 ± 0.0007	22.5 ± 0.8	0.00097 ± 0.00002
C0.41	29.1 ± 2	0.10 ± 0.007	7.86 ± 2.2	0.00035 ± 0.0002

in this equation would not achieve better results. Thus, adsorption on Pt is not expressed explicitly in Eq. [1]. The adsorption constant K_1 is a little higher for C0.41; however, K_2 is 3 times greater for TiO_2. The higher oxidation rates over C0.41 at low acetone concentrations are related to the greater rate constant k_1 and adsorption constant K_1. At higher acetone concentrations, sites of the second type that cause weaker adsorption begin to function. TiO_2 has better kinetic parameters for these sites and provides a higher oxidation rate on them. Thus, comparing the efficiency of platinized and unplatinized titania depends on the concentration. For sample C0.41, the number of Pt atoms on each TiO_2 particle averages 13.5. These atoms probably form one cluster that occupies only a small percentage of the surface of the TiO_2 particle. The influence of this cluster on the kinetic parameters is significantly higher. This implies that the majority of oxidation events take place near or on this cluster, and the drop in k_2 that probably represents reaction on the rest of TiO_2 particle is understandable on the basis of these terms.

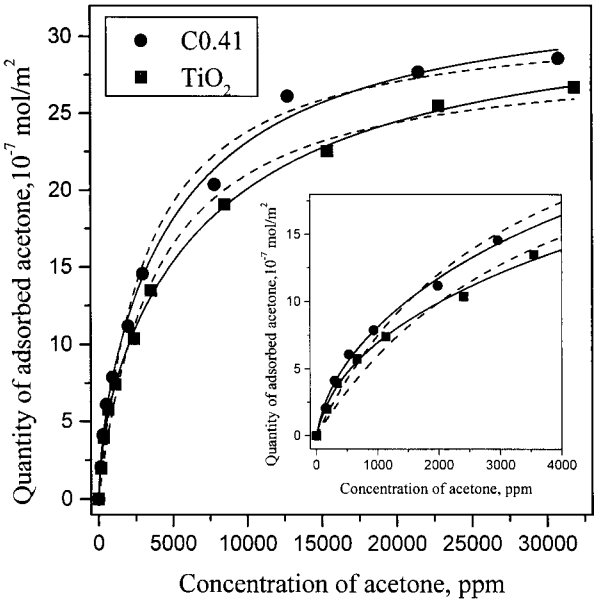

FIG. 9. Isotherms of acetone adsorption on TiO_2 and Pt/TiO_2 C0.41. Water vapor concentration 4000 ppm; temperature 25°C. The inset shows the curves at low acetone concentration.

TABLE 3

Parameters of Acetone Adsorption Isotherms for TiO$_2$ and Pt/TiO$_2$ C0.41 in Fig. 9

Sample	k_1 (10^{-7} mol/m^2)	K_1 (ppm^{-1})	k_2 (10^{-7} mol/m^2)	K_2 (ppm^{-1})
TiO$_2$	5.6 ± 4.2	0.00263 ± 0.00133	27 ± 10	0.00012 ± 0.00002
C0.41	4.8 ± 9.8	0.00377 ± 0.00513	29 ± 23	0.00017 ± 0.00006

Actual isotherms of acetone adsorption on TiO$_2$ and Pt/TiO$_2$ C0.41 are shown in Fig. 9. Solid lines represent fit by a two-site Langmuir adsorption isotherm (expression equal to Eq. [1]), and dashed lines are fit by a one-site Langmuir isotherm. The two-site isotherm describes the isotherms better, especially at low acetone concentration. Parameters of the two-site isotherms are given in Table 3. Adsorption constants calculated from these isotherms are much lower than those calculated from kinetic data. On the first type of sites, the adsorption constant is about 30 times lower, and on the second type of sites, it is 2 times lower. Obviously, UV light stimulates stronger adsorption of acetone. This phenomenon may be similar to the photoadsorption of oxygen. From data in Table 3, total monolayer coverage of acetone was calculated. It is close to 2 molecules/nm^2 for both TiO$_2$ and Pt/TiO$_2$ C0.41. This value is in good agreement with literature data for rutile, 2.61 molecules/nm^2 (27).

Ollis *et al.* (28, 29) studied the kinetics of photocatalytic oxidation of gaseous acetone over TiO$_2$ Degussa P25. Here, we will compare the kinetic parameters of acetone oxidation over TiO$_2$ Degussa P25 and TiO$_2$ of the current study. Ollis *et al.* reported the rate constant $k_0 = 7.75$ mg/(cm^3 of catalyst min) in a plug flow reactor at a water concentration of 1000 ppm, temperature of 22–24°C, and light intensity of $\Phi = 3.5 \times 10^{-7}$ E/(cm^2 min). They used the next form of the LH equation to treat experimental data,

$$R(z) = \nu \frac{dC_a}{dz} = -\frac{k_0 e^{-\alpha \varepsilon z} K C_a(z)}{1 + K C_a(z)}, \qquad [2]$$

where *R(z)* is the rate of oxidation as a function of the catalyst layer depth (mol/(s m^3)), ν is the linear gas velocity through the catalyst layer (cm/s), $\alpha = 0.7$ is the exponent in the dependence of the oxidation rate on light intensity, $R \sim \Phi^{\alpha}$, $\varepsilon = 10211$ cm^{-1} is the effective light absorption coefficient of TiO$_2$, and $C_a(z)$ is the acetone concentration as a function of catalyst layer depth (mg/m^3). In the current study, we use rate constants describing the total rate over catalyst film at a water concentration of 4500 ppm, temperature of 40°C, and light intensity of 1.10×10^{-6} E/(min cm^2). To make a comparison, it is necessary to bring k_0 to the same system of dimensions and conditions. In the flow-circulation reactor, the concentrations are uniform due to a high recirculation rate. If there are no diffusion limitations inside the catalyst film, $C_a(z) = \text{const}$, then the integration of Eq. [2] gives

$$R = \frac{S k_0}{\alpha \varepsilon} \frac{K C_a}{1 + K C_a} = k \frac{K C_a}{1 + K C_a}, \qquad [3]$$

where R is the absolute rate of oxidation (mol/s) and $S = 3.14$ cm^2 is the geometric surface area of the catalyst film. From Eq. [3] the rate constant $k = 9.78 \times 10^{-10}$ mol/s. Now, it is necessary to bring the rate constants to the same conditions. Peral and Ollis (28) reported the light intensity dependence $k(I_2) = k(I_1)(I_2/I_1)^{0.7}$. From this equation, the rate constant at the light intensity of the current study, 1.10×10^{-6} E/(min cm^2), is 21.8×10^{-10} mol/s. To bring the rate constant to the water concentration of the current study, 4500 ppm (6125 mg/m^3), we will use the next equation modified from (28),

$$k(C_2) = k(C_1) \frac{1 + K_H [H_2O]_1^{\beta}}{1 + K_H [H_2O]_2^{\beta}}, \qquad [4]$$

where $K_H = 9.6 \times 10^{-7}$ m^3/mg and $\beta = 1.7$. Thus, k(4500 ppm) $= 3.19 \times 10^{-10}$ mol/s. No temperature dependence was reported for acetone photocatalytic oxidation over Degussa P25. Therefore, we transform our rate constants from 40 to 24°C. In our previous study (12) we reported that two types of sites participate in the photocatalytic oxidation of acetone. The rate constant on sites of the first type, k_1, significantly increases with an increase of temperature, whereas the rate constant on sites of the second type, k_2, does not change markedly with temperature. To calculate the value of k_1 at 24°C, we take the Arrhenius dependence of k_1 on temperature. From the values of k_1 at 40°C (23.8×10^{-10}) and 80°C (36.2×10^{-10} mol/s) the calculations give the pre-exponential factor $k_{10} = 9.61 \times 10^{-8}$ mol/s and apparent activation energy $E_a = 9.6$ kJ/mol. This value is close to the apparent activation energy of acetone photocatalytic oxidation over platinized titania. At 24°C $k_1 = 19.5 \times 10^{-10}$ mol/s. Now, we have the values of rate constants under the same conditions: temperature of 24°C, water concentration of 4500 ppm, and light intensity of 1.10×10^{-6} E/(min · cm^2).

$$k(\text{Degussa P25}) = 3.19 \times 10^{-10} \text{ mol/s},$$
$$k_1(\text{TiO}_2) = 19.5 \times 10^{-10} \text{ mol/s},$$
$$k_2(\text{TiO}_2) = 22.5 \times 10^{-10} \text{ mol/s}.$$

The rate constant on TiO_2 Degussa P25 is over 6 times lower than the rate constants over TiO_2 used in our studies.

Now, we check the accuracy of the assumption of constant acetone concentration in the film of a photocatalyst. From the value of an effective light absorption coefficient of TiO_2 ($\varepsilon = 10211\ cm^{-1}$), we calculated that the characteristic depth of light penetration, L, is about 1×10^{-4} cm. For further estimations we assume that all photocatalytic oxidation takes place at a distance of L from the surface of the TiO_2 layer. From the first Fick's law,

$$\frac{R}{S} = D_e \frac{\Delta C_a}{L}, \qquad [5]$$

where R is the rate or oxidation (mol/s), $S = 3.14\ cm^2$ is the geometric surface area of the catalyst film, D_e is the effective diffusion coefficient (cm^2/s), and ΔC_a is the difference between acetone concentration outside the catalyst film and inside the film at a distance L from the surface. Combining Eqs. [1] and [5] gives

$$\delta = \frac{\Delta C_a}{C_a} \times 100\% = \frac{L}{S D_e} \left(\frac{k_1 K_1}{1 + K_1 C_a} + \frac{k_2 K_2}{1 + K_2 C_a} \right) \times 100\%, \qquad [6]$$

where δ is the relative difference of acetone concentration (%). Taking $D_e = 10^{-4}\ cm^2/s$, we obtain the largest $\delta = (6.7 \times 10^{-9})\%$ at an acetone concentration close to zero. Even if we take a much lower effective diffusion coefficient, the acetone concentration gradient will be negligible. Thus, the above assumption is very accurate and there is no diffusion limitation of the reaction rate.

Ollis *et al.* reported the adsorption constant of acetone on TiO_2 Degussa P25 to be 0.00644 m^3/mg (0.0152 ppm^{-1}) for a water concentration of 1000 ppm (1290 mg/m^3) in a plug flow system (28) and 0.0107 m^3/mg (0.0253 ppm^{-1}) for a water concentration of 14,970 ppm (11,000 mg/m^3) in a monolith system (29). In the current study, adsorption constants on TiO_2 are 0.088 and 0.00097 ppm^{-1} for sites of the first and second types, respectively, at a water concentration of 4500 ppm. However, the one-site LH model gives $K = 0.030\ ppm^{-1}$, which is close to the value obtained for TiO_2 Degussa P25 in the monolith system (29).

For practical applications of photocatalytic oxidation, it is important to have catalysts with very high activity. This can be achieved by optimizing the preparation procedure including optimization of the percentage of platinum. Figure 10 shows the dependence of the acetone oxidation rate on the platinum content at 40°C. In this plot, we took C0.00 as a sample with zero platinum content. The highest reaction rate was found for C0.11. For all these samples, the estimated platinum loading per each TiO_2 particle is rather low and ranges from 2.6 atoms for C0.08 to 25 atoms for C0.76; therefore, it is unlikely that a TiO_2 particle can carry more than one platinum cluster. Failure to observe Pt particles by TEM is corroborated by this estimate since a particle with a diameter of 1 nm, which is close to resolution, consists of approximately 35 atoms. At low platinum percentages, only a fraction of TiO_2 particles may carry Pt clusters. With the increase in the Pt content, more TiO_2 particles carry Pt, which can lead to an increase in photocatalytic activity. The decrease in the activity with the increase in the Pt content may be due to an increasing content of sodium and boron species as well as etching of the TiO_2 surface by chloroplatinic acid (15).

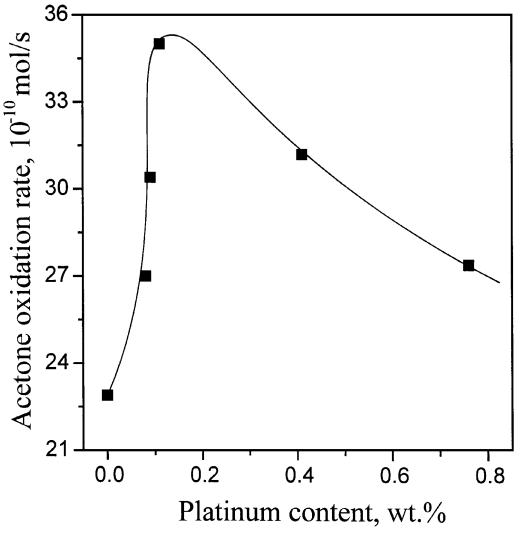

FIG. 10. Plot of acetone oxidation rate vs platinum loading for Pt/TiO_2. Weight of catalysts 30 mg; temperature 40°C; acetone concentration 590 ppm; water vapor concentration 4500 ppm.

CONCLUSION

Deposition of Pt on TiO_2 by photocatalytic and chemical reduction resulted in platinum particles smaller than 1 nm. Platinized titania, prepared by reduction with $NaBH_4$, is more active in complete oxidation of gaseous acetone (500 ppm) than platinized titania prepared by photocatalytic deposition of platinum. Moreover, only samples with chemically deposited platinum were more active than TiO_2. The temperature dependence of the steady state oxidation rate over platinized titania with various platinum loadings does not exhibit temperature deactivation, which is observed over unplatinized TiO_2. The increases in the acetone photocatalytic and thermal oxidation rates over Pt/TiO_2 are well represented by exponential growths. Modification of the TiO_2 surface during platinization can make a significant contribution to the enhanced activity of platinized titania, especially at elevated temperature: TiO_2 treated with $NaBH_4$ showed deactivation only at temperatures above 120°C. Another contribution is anticipated from the photostimulated oxidation of acetone on Pt particles. At 40°C, the higher activity of Pt/TiO_2 is a result of stronger acetone

adsorption and higher rate constant. Of the samples containing from 0.08 to 0.76 wt% Pt, the highest activity at a temperature of 40°C and an acetone concentration of 500 ppm was observed over a sample with 0.11 wt% Pt.

ACKNOWLEDGMENTS

We are grateful to Prof. Jin Zhensheng (College of Chemistry and Chemical Engineering, Henan University, Kaifeng, China) for preparing photoplatinized titania. Generous support by the Russian Federal Program "Integration" is gratefully acknowledged.

REFERENCES

1. Sato, S., and White, J. M., *J. Catal.* **69**, 128 (1981).
2. Yamaguti, K., and Sato, S., *J. Phys. Chem.* **89**, 5510 (1985).
3. Tabata, S., Nishida, H., Masaki, Y., and Tabata, K., *Catal. Lett.* **34**, 245 (1995).
4. Sayama, K., and Arakawa, H., *J. Chem. Soc., Chem. Commun.* 150 (1992).
5. Sato, S., *J. Phys. Chem.* **87**, 3531 (1983).
6. Kudo, A., Domen, K., Maruya, K., and Onishi, T., *Chem. Lett.* 1019 (1987).
7. Malati, M. A., Attubato, L. A., and Beaney, K., *Sol. Energy Mater. Sol. Cells* **40**, 1 (1996).
8. Anpo, M., Aikawa, N., and Kubokawa, Y., *J. Phys. Chem.* **88**, 3998 (1984).
9. Courbon, H., Herrmann, J.-M., and Pichat, P., *J. Catal.* **72**, 129 (1981).
10. Herrmann, J.-M., Courbon, H., and Pichat, P., *J. Catal.* **108**, 426 (1987).
11. Obee, T. N., and Brown, R. T., *Environ. Sci. Technol.* **29**, 1223 (1995).
12. Vorontsov, A. V., Kurkin, E. N., and Savinov, E. N., *J. Catal.* **186**, 318 (1999).
13. Sauer, M. L., Hale, M. A., and Ollis, D. F., *J. Photochem. Photobiol. A: Chem.* **88**, 169 (1995).
14. Jacoby, W. A., Blake, D. M., Noble, R. D., and Koval, C. A., *J. Catal.* **157**, 87 (1995).
15. Kennedy, J. C., III, and Datye, A. K., *J. Catal.* **179**, 375 (1988).
16. Falconer, J. L., and Magrini-Bair, K. A., *J. Catal.* **179**, 171 (1998).
17. Fu, X., Zeltner, W. A., and Anderson, M. A., *Appl. Catal.B: Environ.* **6**, 209 (1995).
18. Nosaka, Y., Koenuma, K., Ushida, K., and Kira, A., *Langmuir* **12**, 736 (1996).
19. Jin, Z., Chen, Z., Li, Q., Xi, C., and Zheng, X., *J. Photochem. Photobiol. A: Chem.* **81**, 177 (1994).
20. Vorontsov, A. V., Savinov, E. N., and Jin, Z., *J. Photochem. Photobiol. A: Chem.* **125**, 113 (1999).
21. Vorontsov, A. V., Savinov, E. N., Barannik, G. B., Troitsky, V. N., and Parmon, V. N., *Catal. Today* **39**, 207(1997).
22. Luo, S., and Falconer, J. L., *J. Catal.* **185**, 393 (1999).
23. Panov, A. G., and Fripiat, J. J., *Catal. Lett.* **57**, 25 (1999).
24. Idriss, H., Kim, K. S., and Barteau, M. A., *J. Catal.* **139**, 119 (1993).
25. Panov, A. G., and Fripiat, J. J., *J. Catal.* **178**, 188 (1998).
26. Chen, B., Close, J. S., and White, J. M., *J. Catal.* **46**, 253 (1977).
27. McClellan, A. L., and Harnsberger, H. F., *J. Colloid Interface. Sci.* **23**, 577 (1967).
28. Peral, J., and Ollis, D. F., *J. Catal.* **136**, 554 (1992).
29. Sauer, M. L., and Ollis, D. F., *J. Catal.* **149**, 81 (1994).